Inelastic Electron Tunneling Spectroscopy of Gold−Benzenedithiol−Gold Junctions: Accurate Determination of Molecular Conformation

Li-Li Lin,[†,‡] Chuan-Kui Wang,[†] and Yi Luo[‡,§,*]

[†]College of Physics and Electronics, Shandong Normal University, Jinan 250014, P.R. China, [‡]Department of Theoretical Chemistry, School of Biotechnology, Royal Institute of Technology, S-10691 Stockholm, Sweden, and [§]Hefei National Laboratory for Physical Sciences at the Microscale, University of Science and Technogy of China, 230026, Hefei, China

ABSTRACT The gold−benzenedithiol−gold junction is the classic prototype of molecular electronics. However, even with the similar experimental setup, it has been difficult to reproduce the measured results because of the lack of basic information about the molecular confirmation inside the junction. We have performed systematic first principles study on the inelastic electron tunneling spectroscopy of this classic junction. By comparing the calculated spectra with four different experimental results, the most possible conformations of the molecule under different experimental conditions have been successfully determined. The relationship between the contact configuration and the resulted spectra is revealed. It demonstrates again that one should always combine the theoretical and experimental inelastic electron tunneling spectra to determine the molecular conformation in a junction. Our simulations have also suggested that in terms of the reproducibility and stability, the electromigrated nanogap technique is much better than the mechanically controllable break junction technique.

KEYWORDS: inelastic electron tunneling · molecular junctions · molecular conformations · density functional theory · vibrations

Since the pioneering work of Reed *et al.*[1] in 1997, the gold−benzenedithiol−gold (Au−BDT−Au) molecular junction has been the subject of extensive experimental and theoretical investigations, aiming to understand the basic nature of the electron transport in a molecular device.[2−32] During many years, the reported experimental conductance values vary by almost 4 orders of magnitude from different research groups and are very difficult to be reproduced by theoretical calculations. One of the major reasons for such problems is the lack of detailed information about the molecular conformation and the contact geometry in actual junctions.[14−32] Although the atom-resolved observation of the molecular junction is still out of reach at this stage, the inelastic electron tunneling spectroscopy (IETS) technique can provide experimentally indirect structural information through the response of the molecular vibrations.[33,34] In recent years, the IETS technique has been successfully applied to a number of molecular junctions and proved to be a powerful tool to verify the actual presence of the molecule and to extract the geometric information in the molecular junction.[35−46]

Although Au−BDT−Au is probably the simplest and most studied molecular junction, its IETS spectra have only become available very recently.[47−50] There are four reported IETS spectra with very different spectral profiles, which were obtained for junctions made from the electromigrated nanogap technique[47,50] and mechanically controllable break junction (MCBJ),[48,49] respectively. From these experimental spectra, it can be ensured that there are indeed molecules within the junction and the molecule could have very different conformation in different junctions. But the experiments alone can neither determine the exact conformation of the molecule inside the junction nor tell what the structural difference is among different junctions. The aim of this study is thus to establish the possible structure-to-spectrum relationship for the IETS of the Au−BDT−Au junction and to determine the exact molecular conformation by comparing theoretical and experimental spectra.

RESULTS AND DISCUSSION

The simplest model for the IETS of the molecular junction is to only consider the

* Address correspondence to luo@kth.se.

Received for review December 18, 2010 and accepted February 2, 2011.

Published online February 10, 2011
10.1021/nn103522k

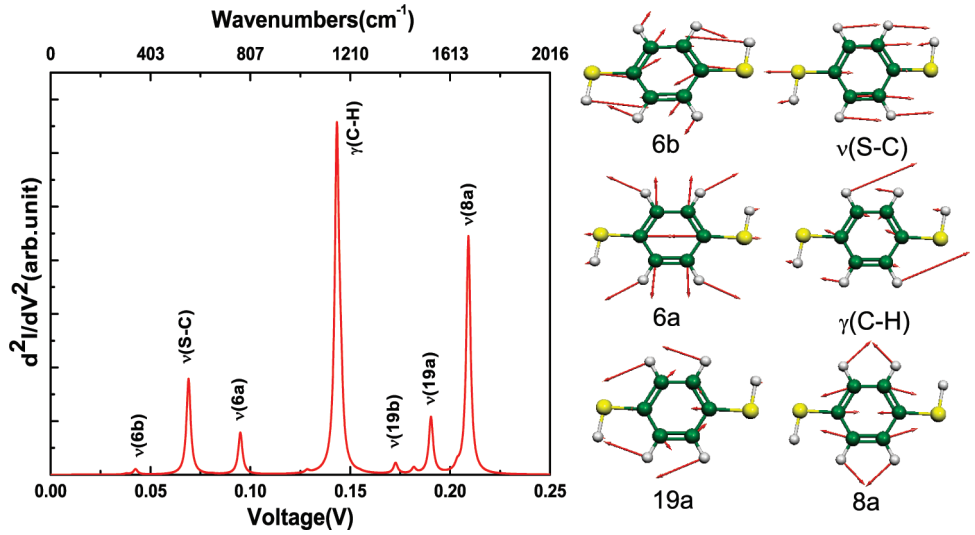

Figure 1. The IETS of the BDT molecule in gas phase. The important vibration modes with considerable intensity are assigned. The Lorentzian line shape is adopted, and the broadening factor for the calculated spectrum is set to 10 cm^{-1}.

molecule itself, in this case the coupling between the molecule and the metal contacts is set to be a constant. This approach was used by Troisi *et al.*[56−58] and revealed many interesting features of the IETS. The calculated IETS spectrum of the BDT molecule is given in Figure 1, on which the vibrational modes with visible intensity are identified. It can be clearly seen that the C−H in-plane bending (γ(C−H)) and the C═C in-plane stretching (ν(8*a*)) modes dominate the spectrum. Several other modes also have considerable intensity. We will show here that the presence of an actual metal electrode can have significant effects on the IETS of the molecular junction.

We have done a systematic study on the IETS of the Au−BDT−Au junction with many different configurations. Here we will only discuss some basic features of the IETS and the calculated spectra that are comparable with the experimental ones.

We start with a typical configuration TT as shown in Figure 2I, where both sulfur atoms are located at the top site of two gold electrodes. In this case, the S−S axis has an angle of 26.8 degree with respect to the normal of the electrode. We have calculated the energy profile as a function of the width of the junction. It is found that the molecular junction becomes stable when the electrode distance is around 1.21 nm and the distance between the sulfur atom and the electrode is 0.32 nm. It should be noted that the stable structure determined for such an ideal system might not be the one in the real device due to the possible influences of the temperature and the surroundings. In addition, the gold surface is assumed to be rigid without geometric fluctuations. The use of IETS is thus necessary and useful. The calculated IETS spectra of the TT junction with the width of 1.03 nm, 1.11 nm, 1.19 nm, and 1.27 nm, respectively, are shown in Figure 2II. One can immediately see that the IETS is very sensitive to the change of the electrode distance. It is known that the vibrational modes at low frequencies in the IET spectra correspond to the motions of the gold atoms. When the width is 1.11 nm, the first peak at the low frequency region becomes relatively weak. Compared with the spectrum in the gas phase, one can notice that the S−Au stretching mode shows up at about 0.04 V in the TT junction and the red-shift of other peaks can also be observed owing to the influence of the gold electrode. The C−H in-plane bending (γ(C−H)) and the C═C in-plane stretching (ν(8*a*)) dominant in the gas phase are somehow suppressed in the TT contact configuration because of the presence of the S−Au stretching mode. This is a direct result of the competition between two different pathways: one is through the S−Au bond, while another is through the C−H bond close to the electrode bypassing the S−Au bond. When the S−Au bonding becomes strong, the electrons will prefer to tunnel through the S−Au bond rather than go though the C−H bond to the electrodes; consequently, the C−H in-plane bending mode and the C═C in-plane stretching mode become relatively weaker.

The junction could also be formed in an asymmetric fashion and one of the examples is the configuration BT as illustrated in Figure 2III, in which one sulfur atom is located at the top of the electrode and another is at the bridge of the electrode. Here, the S−S axis has an angle of 13° with respect to the normal of the electrode. The energy profile of the molecule in the BT configuration as the function of the junction width is given in Figure 2III. For such a configuration, the steady point is at the width of about 1.25 nm and the sulfur-electrode distance becomes 0.31 nm, which are very similar to the TT configuration. It is also found that the total energy of the BT junction is only 0.025 eV higher than that of the TT junction. Therefore, both configurations

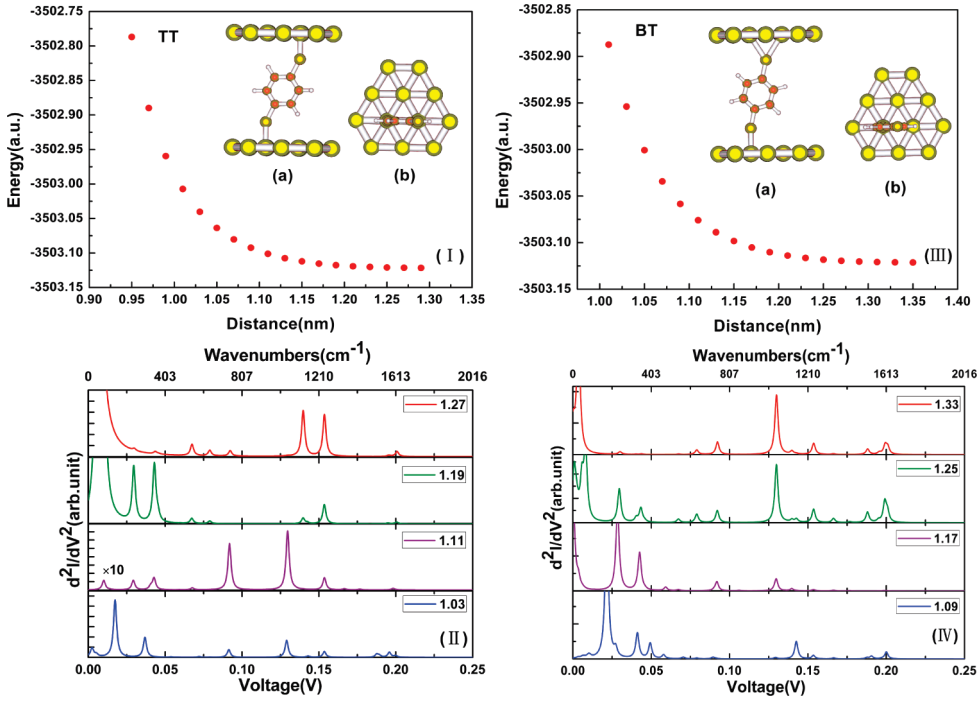

Figure 2. (I) Variation of the total energy of the extended BDT molecule with the TT contact configuration ((a) side view and (b) top view in the insert) as the function of the junction width; (II) IETS of the TT junctions with different width, while the intensity of the peak at low frequency in the purple line is amplified by 10 times to make it visible; (III) variation of the total energy of the extended BDT molecule with the BT contact configuration ((a) side view and (b) top view in the insert) as the function of the junction width; (IV) IETS of the BT junctions with different width. The Lorentzian line shape is adopted and the broadening factor for the calculated spectrum is set to 10 cm^{-1}.

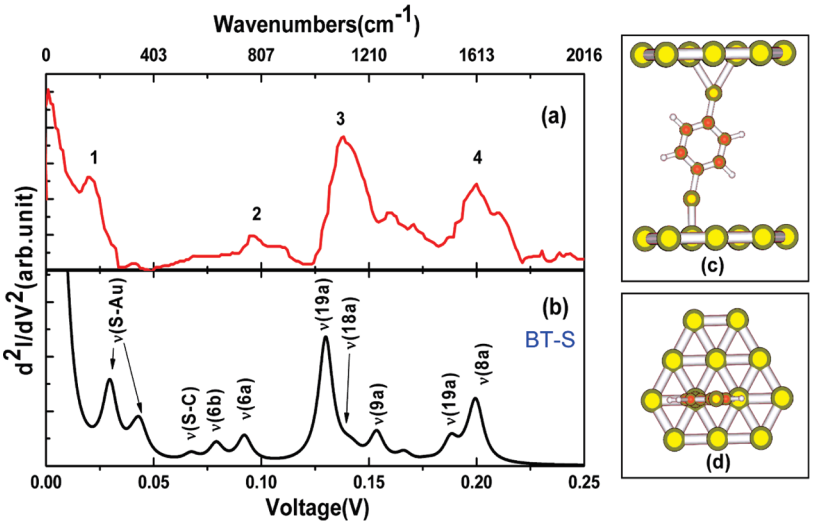

Figure 3. (a) Experimental[47] and (b) calculated IETS spectrum of the BT-S molecular junction with the electrode distance of 1.25 nm. The side view (c) and the top view (d) of the BT-S junction. The Lorentzian line shape is adopted and the broadening factor for the calculated spectrum is set to 32 cm^{-1}.

could occur in reality from the energetic point of view. The calculated IETS spectra of the BT junction with the electrode distance of 1.09, 1.17, 1.25, and 1.33 nm are displayed in Figure 2IV. It is found that the intensity of the S−Au mode becomes weaker with the increase of the junction width and the other vibrational modes gets stronger, in particular, the vibrational mode at about 0.13 V gradually dominates. By comparing with the calculated spectra of the TT junctions, it can be seen that the contact geometry can also have significant effects on the IETS spectrum.

It is interesting to note that the BT junction is capable of reproducing one of the experimental results for the Au−BDT−Au junction. To highlight the good agreement, the calculated spectrum with the width of 1.25 nm (BT-S) is shown in Figure 3 together with the experimental

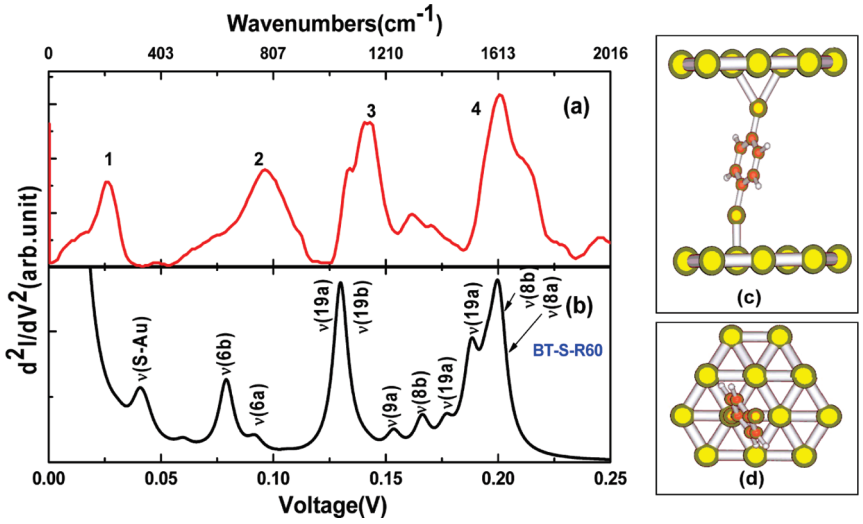

Figure 4. (a) Experimental[50] and (b) the calculated IETS spectra of the BT-S-R60 junction. The side view (c) and the top view (d) of the BT-S-R60 junction. The Lorentzian line shape is adopted and the broadening factor for the calculated spectra is set to 32 cm^{-1}.

spectrum of Song *et al.*[47] There are four peaks in the spectra with the third one dominating, which is attributed from the C−H in-plane bending modes $\nu(18a)$ and $\nu(19a)$. It can be seen that the C═C stretching modes $\nu(8a)$ and $\nu(19a)$ contribute to the fourth peak, while the second peak consists of a group of vibration modes, such as C−C−C bending modes $\nu(6a)$ and $\nu(6b)$, as well as the S−C stretching mode $\nu(S-C)$.

When the molecule is rotated 60° with respect to the S−S axis in the BT-S junction, it is found that the calculated spectrum for this conformation (BT-S-R60) can reproduce another experimental spectrum also measured by Song *et al.* at the same temperature (4.2 K) with the same technique,[50] as demonstrated in Figure 4a,b. The intensity of the spectral peak in the experimental spectrum follows the relationship: 1(127) < 2(97) < 3(141) < 4(199 mV). Our theoretical simulation gives the same trend though there is slight mismatch in the peak positions. All the vibrational modes observed in the experiments have been assigned. It shows that the C═C stretching modes $\nu(8a)$ and $\nu(8b)$ dominate the spectrum. Compared with the IETS spectrum for the BT-S junction measured (in Figure 3a), peak 4 becomes stronger and peak 1 becomes weaker, which is a direct consequence of the molecular rotation. In general, the C═C stretching modes and C−H in-plane bending modes at high frequencies seem to compete to be the dominant contributor. This could be understood since the IETS is strongly associated with the pathway of the electron tunneling through the molecule.[59] The BT-S-R60 and the BT-S junctions have exactly the same molecular structure, junction width, and contact. The only difference is the mutual orientation between the molecule and the electrodes. Our calculation shows that there is almost no barrier for the BDT molecule to rotate around its S−S axis. It is thus possible to obtain junctions with different rotation angles in the experiments. This partially explains why with the exactly the same experimental technique and conditions, the generated junctions could have very different IETS spectra.

With a further rotation of the molecule around the S−S axis to 90° (BT-S-R90), the calculated spectrum seems to resemble the experimental spectrum measured by Tsutsui *et al.*[49] with the break junction technique. In particular, when the junction width is increased to 1.29 nm, the calculated spectrum for this widened junction, BT-S-R90-W, is in good agreement with the experiment, as illustrated in Figure 5a,b. In comparison with the result for the junction BT-S-R90 in Figure 5c, the relative intensity of the S−Au modes becomes weaker. In general, the spectrum for this junction shows more structures. We can assign peak 4 to the C═C stretching mode $\nu(8a)$ and the C−H in-plane bending mode $\nu(19a)$. Peak 3 mainly comes from the C−H in-plane stretching modes including $\nu(18a)$, $\nu(19a)$, and $\nu(18b)$. In the peak 2, both C−C−C bending mode $\nu(6b)$ and $\nu(6a)$ can be found. Comparing with the spectra measured by Song *et al.* for the junction made from the electromigrated nanogap technique,[47,50] the most significant change is the increasing intensity of the S−Au mode. This indicates that in this case the pathway through the S−Au bond is more favorable for electron transport.

Although both the electromigrated nanogap and the mechanically controllable break junction techniques can not guarantee production of the junctions of the same property, the electromigrated nanogap seems to be a better one in terms of reproducibility, since the difference in the products is mainly the rotation angle as revealed by our simulations presented here. By simply changing one structural parameter, we find it impossible to reproduce another experimental IETS spectrum from the mechanically controllable break junction technique.[48] With the experience we have gained from the simulations of

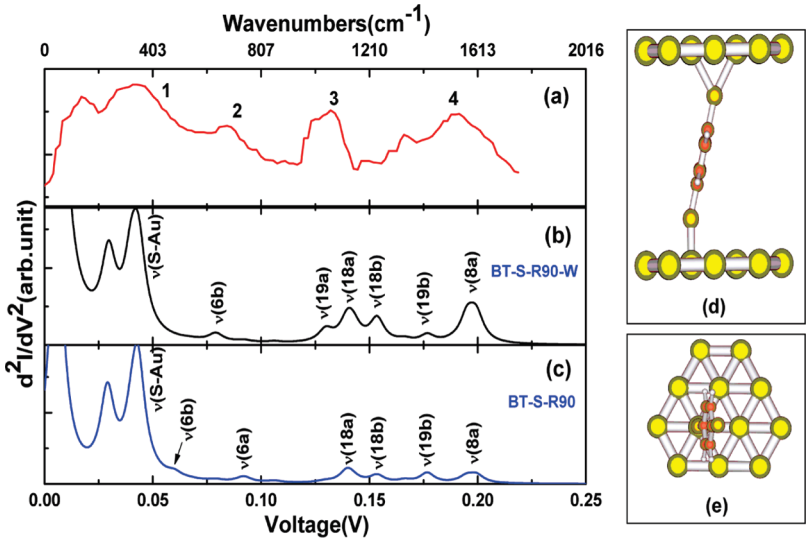

Figure 5. (a) Experimental[49] and (b) the calculated IETS spectra of the BT-S-R90-W junction with the width of 1.29 nm, in comparison with that (c) for the BT-S-R90 with the width of 1.25 nm. The side view (d) and the top view (e) of the BT-S-R90-W junction. The Lorentzian line shape is adopted and the broadening factor for the calculated spectra is set to 32 cm^{-1}.

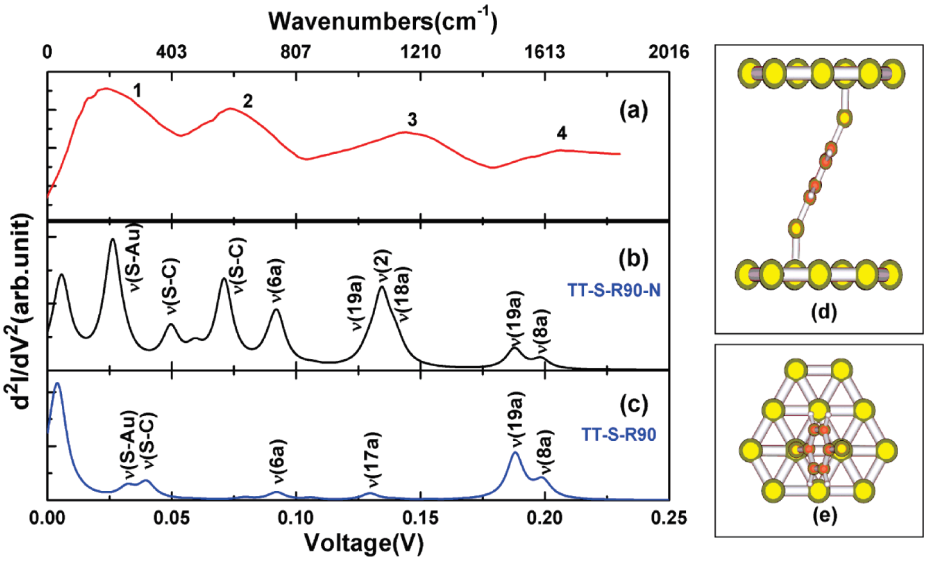

Figure 6. (a) Experimental[48] and (b) calculated IETS spectra of the TT-S-R90-N junction with the width of 1.07 nm, in comparison with that (c) for the TT-S-R90 with the width of 1.25 nm. The side view (d) and the top view (e) of the TT-S-R90-N junction. The Lorentzian line shape is adopted and the broadening factor for the calculated spectra is set to 32 cm^{-1}.

different junctions, we could identify a junction that can give the IETS spectrum in good agreement with the experiment, as illustrated in Figure 6a,b. This junction is of a TT type as shown in Figure 2l, but is rotated with a 90° around the S−S axis and has a width of only 1.07 nm, which is about 0.18 nm narrower than the normal BT-S junctions. Such a narrow junction, TT-S-R90-N, has a quite different spectral profile. The four major peaks in the experiment obeys the order 1(35) > 2(81) > 3(153) > 4(207 mV), which is completely reversed in comparison with the experimental result measured by Song *et al.*[50] For the TT-S-R90-N junction, the S−C stretching mode becomes an important contributor to peak 2, which implies that the major transport pathway goes through the sulfur atom to the electrode. A comparison with the spectrum of the TT-S-R90 in Figure 6c shows that the larger bond length of S−Au results in weaker intensity from the S−Au vibration modes. It again indicates that the S−Au distance can significantly influence the intensity of the S−Au stretching mode in the IETS spectrum.[41]

Our simulations have now successfully reproduced all four available experimental spectra and revealed the detailed structural information of different devices. It is known that these four experimental spectra were generated from devices made by two different experimental techniques, namely the electromigrated nanogap[47,50] and mechanically controllable break junction.[48,49] Our calculations seem to suggest that the electromigrated nanogap technique is a better technique

in terms of reproducibility. It is found that although the two IETS spectra from the electromigrated nanogap technique have quite different profiles, the devices have almost identical structure and can only be distinguished by the molecular rotation angle along the S−S axis. This technique seems to favor the molecule binding to the two electrodes asymmetrically (the top and the bridge sites, respectively) in all the devices.[47,50] On the other hand, the mechanically controllable break junction technique[48,49] is not capable of accurately determining the bonding site and the contact geometry. The two IETS spectra of the junctions made by the mechanically controllable break junction technique are found to be associated with two very different structures. In one junction, the molecule is symmetrically located at the top sites of the two electrodes; whereas in another junction, the molecule is asymmetrically located at the top and at the bridge of the two electrodes, respectively. Two junctions have also very different junction widths.

SUMMARY

We have shown again the power of the first principles simulations for the IETS spectra of the molecular junctions. Theoretical modeling allows a reproduction of different experimental spectra and more importantly suggests the underlying structural information that is not accessible in the experiments.

THEORETICAL METHOD

Our calculation scheme is based on our early developed quantum chemical approach for the electron transport in molecular junctions,[10,51] in which the effects of the vibronic coupling are treated analytically based on a harmonic approximation and Green's function approach.[38,51] Our method has been shown to be particularly useful for the modeling of IETS.[38−43,51] Since the calculated spectra can often accurately reproduce their experimental counterparts, it thus becomes a powerful means to reveal detailed structural information that is inaccessible in experiments, for instance the molecular conformations inside the junction,[38−40] the molecule−metal contact structures,[41] the intermolecular interaction,[52] the effect of the environment,[53] and the switching mechanism.[42]

In the simulations, 12 gold atoms are used to represent each electrode with a fixed Au−Au bond of 2.88 Å. The molecule was first optimized in the gas phase, then connected to the two gold electrodes through the end sulfur atoms. Different contact configurations including the top, the hollow, and the bridge sites have been considered. For each contact configuration, the electronic structure and the vibrational frequencies of the extended molecule at different electrode distance have been calculated. The distance between the end sulfur atom and the electrode is adjusted by changing the width of the junction. The geometry optimization, the vibrational frequencies, and the electronic structure of the junctions are calculated at the B3LYP level with LanL2DZ basis sets as implemented in Gaussian 03 program.[54] All the IETS calculations are carried out with the QCME program.[55]

Acknowledgment. This work is supported by the Nature Science Foundation of Shandong Province under Grant No. ZR2010AZ002, the National Natural Science Foundation of China (Grant Nos. 10804064, 10974121, and 20925311), the National Basic Research Program of China (2010CB923300), the Swedish Research Council (VR), and the Swedish National Infrastructure for Computing (SNIC). Lin thanks the financial support of China Scholarship Council.

REFERENCES AND NOTES

1. Reed, M. A.; Zhou, C.; Muller, C. J.; Burgin, T. P.; Tour, J. M. Conductance of a Molecular Junction. *Science* **1997,** *278*, 252–254.
2. Yaliraki, S. N.; Roitberg, A. E.; Gonzalez, C.; Mujica, V.; Ratner, M. A. The Injecting Energy at Molecule/Metal Interfaces: Implications for Conductance of Molecular Junctions from an *ab Initio* Molecular Description. *J. Chem. Phys.* **1999,** *111*, 6997–7002.
3. Hall, L. E.; Reimers, J. R.; Hush, N. S.; Silverbrook, K. Formalism, Analytical Model, and *a Priori* Green's-Function-Based Calculations of the Current−Voltage Characteristics of Molecular Wires. *J. Chem. Phys.* **2000,** *112*, 1510–1521.
4. Damle, P.; Ghosh, A. W.; Datta, S. First-Principles Analysis of Molecular Conduction Using Quantum Chemistry Software. *Chem. Phys.* **2002,** *281*, 171–187.
5. Alexandrov, A. S.; Bratkovsky, A. M. Memory Effect in a Molecular Quantum Dot with Strong Electron−Vibron Interaction. *Phys. Rev. B* **2003,** *67*, 235312–235319.
6. Stokbro, K.; Taylor, J.; Brandbyge, M.; Mozos, J. L.; Ordejon, P. Theoretical Study of the Nonlinear Conductance of Di-thiol Benzene Coupled to Au (111) Surfaces *via* Thiol and Thiolate Bonds. *Comput. Mater. Sci.* **2003,** *27*, 151–160.
7. Xu, B. Q.; Tao, N. J. Measurement of Single-Molecule Resistance by Repeated Formation of Molecular Junctions. *Science* **2003,** *301*, 1221–1223.
8. Xiao, X. Y.; Xu, B. Q.; Tao, N. J. Measurement of Single Molecule Conductance: Benzenedithiol and Benzenedimethanethiol. *Nano Lett.* **2004,** *4*, 267–271.
9. Wang, C. K.; Luo, Y. Current−Voltage Characteristics of Single Molecular Junction: Dimensionality of Metal Contacts. *J. Chem. Phys.* **2003,** *119*, 4923–4928.
10. Wang, C. K.; Fu, Y.; Luo, Y. A Quantum Chemistry Approach for Current−Voltage Characterization of Molecular Junctions. *Phys. Chem. Chem. Phys.* **2001,** *3*, 5017–5023.
11. Venkataraman, L.; Klare, J. E.; Tam, I. W.; Nuckolls, C.; Hybertsen, M. S.; Steigerwald, M. L. Single-Molecule Circuits with Well-Defined Molecular Conductance. *Nano Lett.* **2006,** *6*, 458–462.
12. Horiguchi, K.; Tsutsui, M.; Kurokawa, S.; Sakai, A. Electron Transmission Characteristics of Au/1,4-Benzenedithiol/Au Junctions. *Nanotechnology* **2009,** *20*, 025204–025210.
13. Pu, Q.; Leng, Y. S.; Zhao, X. C.; Cummings, P. T. Molecular Simulation Studies on the Elongation of Gold Nanowires in Benzenedithiol. *J. Phys. Chem. C* **2010,** *114*, 10365–10372.
14. Di Ventra, M.; Pantelides, S. T.; Lang, N. D. First-Principles Calculation of Transport Properties of a Molecular Device. *Phys. Rev. Lett.* **2000,** *84*, 979–982.
15. Emberly, E. G.; Kirczenow, G. The Smallest Molecular Switch. *Phys. Rev. Lett.* **2003,** *91*, 188301–188304.
16. Bratkovsky, A. M.; Kornilovitch, P. E. Effects of Gating and Contact Geometry on Current through Conjugated Molecules Covalently Bonded to Electrodes. *Phys. Rev. B* **2003,** *67*, 115307–115313.
17. Xue, Y. Q.; Ratner, M. A. Microscopic Study of Electrical Transport through Individual Molecules with Metallic Contacts. I. Band Lineup, Voltage Drop, and High-Field Transport. *Phys. Rev. B* **2003,** *68*, 115406–115423.
18. Basch, H.; Ratner, M. A. Molecular Binding at Gold Transport Interfaces. III. Field Dependence of Electronic Properties. *J. Chem. Phys.* **2003,** *119*, 11926–11935.

19. Xue, Y. Q.; Ratner, M. A. End Group Effect on Electrical Transport through Individual Molecules: A Microscopic Study. *Phys. Rev. B* **2004,** *69*, 85403–85407.
20. Ke, S. H.; Baranger, H. U.; Yang, W. T. Molecular Conductance: Chemical Trends of Anchoring Groups. *J. Am. Chem. Soc.* **2004,** *126*, 15897–15904.
21. Nara, J.; Geng, W. T.; Kino, H.; Kobayashi, N.; Ohno, T. Theoretical Investigation on Electron Transport through an Organic Molecule: Effect of the Contact Structure. *J. Chem. Phys.* **2004,** *121*, 6485–6492.
22. Geng, W. T.; Nara, J.; Ohno, T. Impacts of Metal Electrode and Molecule Orientation on the Conductance of a Single Molecule. *Appl. Phys. Lett.* **2004,** *85*, 5992–5994.
23. Ke, S. H.; Baranger, H. U; Yang, W. T. Contact Atomic Structure and Electron Transport through Molecules. *J. Chem. Phys.* **2005,** *122*, 074704–074711.
24. Basch, H.; Cohen, R.; Ratner, M. A. Interface Geometry and Molecular Junction Conductance: Geometric Fluctuation and Stochastic Switching. *Nano Lett.* **2005,** *5*, 1668–1675.
25. Tsutsui, M.; Teramae, Y.; Kurokawa, S.; Sakai, A. High-Conductance States of Single Benzenedithiol Molecules. *Appl. Phys. Lett.* **2006,** *89*, 163111–163114.
26. Kondo, H.; Kino, H.; Nara, J.; Ozaki, T.; Ohno, T. Contact-Structure Dependence of Transport Properties of a Single Organic Molecule between Au Electrodes. *Phys. Rev. B* **2006,** *73*, 235323–235332.
27. Zhao, X. C.; Leng, Y. S.; Cummings, P. T. Self-Assembly of 1,4-Benzenedithiolate/Tetrahydrofuran on a Gold Surface: A Monte Carlo Simulation Study. *Langmuir* **2006,** *22*, 4116–4124.
28. Ulrich, J.; Esrail, D.; Pontius, W.; Venkataraman, L.; Millar, D.; Doerrer, L. H. Variability of Conductance in Molecular Junctions. *J. Phys. Chem. B* **2006,** *110*, 2462–2466.
29. Andrews, D. Q.; Cohen, R.; Van Duyne, R. P.; Ratner, M. A. Single Molecule Electron Transport Junctions: Charging and Geometric Effects on Conductance. *J. Chem. Phys.* **2006,** *125*, 174718–174726.
30. Bai, P.; Li, E. P.; Chong, C. C.; Chen, Z. K. Effects of Metal−Molecule Interface Conformations on the Electron Transport of Single Molecule. *Curr. Appl. Phys.* **2006,** *6*, 531–535.
31. Andrews, D. Q.; Van Duyne, R. P.; Ratner, M. A. Stochastic Modulation in Molecular Electronic Transport Junctions: Molecular Dynamics Coupled with Charge Transport Calculations. *Nano Lett.* **2008,** *8*, 1120–1126.
32. Malen, J. A.; Doak, P.; Baheti, K.; Tilley, T. D.; Majumdar, A.; Segalman, R. A. The Nature of Transport Variations in Molecular Heterojunction Electronics. *Nano Lett.* **2009,** *9*, 3406–3412.
33. Gagliardi, A.; Solomon, G. C.; Pecchia, A.; Frauenheim, T.; Di Carlo, A.; Hush, N. S.; Reimers, J. R. *A Priori* Method for Propensity Rules for Inelastic Electron Tunneling Spectroscopy of Single-Molecule Conduction. *Phys. Rev. B* **2007,** *75*, 174306–174313.
34. Beebe, J. M.; Moore, H. J.; Lee, T. R.; Kushmerick, J. G. Vibronic Coupling in Semifluorinated Alkanethiol Junctions: Implications for Selection Rules in Inelastic Electron Tunneling Spectroscopy. *Nano Lett.* **2007,** *7*, 1364–1368.
35. Smit, R. H. M.; Noat, Y.; Untiedt, C.; Lang, N. D.; Van Hemert, M. C.; Van Ruitenbeek, J. M. Measurement of the Conductance of a Hydrogen Molecule. *Nature* **2002,** *419*, 906–909.
36. Wang, W. Y.; Lee, T.; Kretzschmar, I.; Reed, M. A. Inelastic Electron Tunneling Spectroscopy of an Alkanedithiol Self-Assembled Monolayer. *Nano Lett.* **2004,** *4*, 643–646.
37. Kushmerick, J. G.; Lazorcik, J.; Patterson, C. H.; Shashidhar, R.; Seferos, D. S.; Bazan, G. C. Vibronic Contributions to Charge Transport across Molecular Junctions. *Nano Lett.* **2004,** *4*, 639–642.
38. Jiang, J.; Kula, M.; Lu, W.; Luo, Y. First-Principles Simulations of Inelastic Electron Tunneling Spectroscopy of Molecular Electronic Devices. *Nano Lett.* **2005,** *5*, 1551–1555.
39. Leng, J. C.; Lin, L. L.; Song, X. N.; Li, Z. L.; Wang, C. K. Orientation of Decanethiol Molecules in Self-Assembled Monolayers Determined by Inelastic Electron Tunneling Spectroscopy. *J. Phys. Chem. C* **2009,** *113*, 18353–18357.
40. Lin, L. L.; Song, X. N.; Leng, J. C.; Li, Z. L.; Luo, Y.; Wang, C. K. Determination of the Configuration of a Single Molecule Junction by Inelastic Electron Tunneling Spectroscopy. *J. Phys. Chem. C* **2010,** *114*, 5199–5202.
41. Kula, M.; Jiang, J.; Luo, Y. Probing Molecule−Metal Bonding in Molecular Junctions by Inelastic Electron Tunneling Spectroscopy. *Nano Lett.* **2006,** *6*, 1693–1698.
42. Cao, H.; Jiang, J.; Ma, J.; Luo, Y. Identification of Switching Mechanism in Molecular Junctions by Inelastic Electron Tunneling Spectroscopy. *J. Phys. Chem. C* **2008,** *112*, 11018–11022.
43. Jiang, J.; Kula, M.; Luo, Y. Molecular Modeling of Inelastic Electron Transport in Molecular Junctions. *J. Phys.: Condens. Matter* **2008,** *20*, 374110–374121.
44. Vitali, L.; Ohmann, R.; Kern, K.; Garcia-Lekue, A.; Frederiksen, T.; Sanchez-Portal, D.; Arnau, A. Surveying Molecular Vibrations during the Formation of Metal−Molecule Nanocontacts. *Nano Lett.* **2010,** *10*, 657–660.
45. Arroyo, C. R.; Frederiksen, T.; Rubio-Bollinger, G.; Velez, M.; Arnau, A.; Sanchez-Portal, D.; Agrait, N. Characterization of Single-Molecule Pentanedithiol Junctions by Inelastic Electron Tunneling Spectroscopy and First-Principles Calculations. *Phys. Rev. B* **2010,** *81*, 075405–075409.
46. Gagliardi, A.; Solomon, G. C.; Pecchia, A.; Di Carlo, A.; Frauenheim, T.; Reimers, J. R.; Hush, N. S. Simulations of Inelastic Tunnelling in Molecular Bridges. Nonequilibrium Carrier Dynamics in Semiconductors: Proceedings of the 14th International Conference, July 25-29, 2005, Chicago, Il.; Springer Proceedings in Physics;Springer: Berlin, 2006; Vol. 110, pp 183−186.
47. Song, H.; Kim, Y.; Jang, Y. H.; Jeong, H.; Reed, M. A.; Lee, T. Observation of Molecular Orbital Gating. *Nature* **2009,** *462*, 1039–1043.
48. Taniguchi, M.; Tsutsui, M.; Yokota, K.; Kawai, T. Inelastic Electron Tunneling Spectroscopy of Single-Molecule Junctions Using a Mechanically Controllable Break Junction. *Nanotechnology* **2009,** *20*, 434008–434015.
49. Tsutsui, M.; Taniguchi, M.; Shoji, K.; Yokota, K.; Kawai, T. Identifying Molecular Signatures in Metal−Molecule−Metal Junctions. *Nanoscale* **2009,** *1*, 164–170.
50. Song, H.; Kim, Y.; Ku, J.; Jang, Y. H.; Jeong, H.; Lee, T. Vibrational Spectra of Metal−Molecule−Metal Junctions in Electromigrated Nanogap Electrodes by Inelastic Electron Tunneling. *Appl. Phys. Lett.* **2009,** *94*, 103110–103112.
51. Jiang, J.; Kula, M.; Luo, Y. A Generalized Quantum Chemical Approach for Elastic and Inelastic Electron Transports in Molecular Electronics Devices. *J. Chem. Phys.* **2006,** *124*, 034708–034717.
52. Kula, M.; Luo, Y. Effects of Intermolecular Interaction on Inelastic Electron Tunneling Spectra. *J. Chem. Phys.* **2008,** *128*, 064705–064711.
53. Kula, M.; Jiang, J.; Lu, W.; Luo, Y. Effects of Hydrogen Bonding on Current−Voltage Characteristics of Molecular Junctions. *J. Chem. Phys.* **2006,** *125*, 194703–194709.
54. Frisch, M. J.; Trucks, G. W.; Schlegel, H. B.; Scuseria, G. E.; Robb, M. A.; Cheeseman, J. R.; Montgomery, J. A., Jr.; Vreven, T.; Kudin, K. N.; Burant, J. C.; *et al. Gaussian 03,* revision C 02, Gaussian, Inc.: Wallingford, CT, 2004; p 5.
55. Jiang J; Wang C. -K.; Luo Y.; *Quantum Chemistry for Molecular Electronics (QCME-V1.1)*, Royal Institute of Technology, Sweden, 2006.
56. Troisi, A.; Ratner, M. A.; Nitzan, A. Vibronic Effects in Off-Resonant Molecular Wire Conduction. *J. Chem. Phys.* **2003,** *118*, 6072–6082.
57. Troisi, A.; Ratner, M. A. Modeling the Inelastic Electron Tunneling Spectra of Molecular Wire Junctions. *Phys. Rev. B* **2005,** *72*, 33408–33411.
58. Troisi, A.; Ratner, M. A. Propensity Rules for Inelastic Electron Tunneling Spectroscopy of Single-Molecule Transport Junctions. *J. Chem. Phys.* **2006,** *125*, 214709–214719.
59. Troisi, A.; Beebe, J. M.; Picraux, L. B.; Van Zee, R. D.; Stewart, D. S.; Ratner, M. A.; Kushmerick, J. G. Tracing Electronic Pathways in Molecules by Using Inelastic Tunneling Spectroscopy. *Proc. Natl. Acad. Sci. U.S.A.* **2007,** *104*, 14255–14259.